J. Synchrotron Rad. (1998). **5**, 609–611

Allowable aperture size of the front end for the high-heat-load undulator beamlines of SPring-8

M. Oura,* H. Sakae,† Y. Sakurai and H. Kitamura

JAERI-RIKEN SPring-8 Project Team, Kamigori, Ako-gun, Hyogo 678-12, Japan. E-mail: oura@sp8sun.spring8.or.jp

(*Received 4 August 1997; accepted 12 November 1997*)

A systematic study to determinine the allowable aperture size of the front end for the SPring-8 high-heat-load undulator beamlines has been performed, from the viewpoint of protecting the front-end Be window from thermomechanical failure, and based on the results of ANSYS finite-element analyses. These results have revealed that the allowable aperture size of the front end ranges approximately from 1.06 mm^2 to 3.2 mm^2 depending on the K-parameter and the filter thickness.

Keywords: front ends; high-heat-load components; thermomechanical analysis of Be windows.

1. Introduction

The SPring-8 standard in-vacuum undulator, whose magnetic period length is 32 mm and number of periods is 140, radiates extremely high-heat-load radiation (Kitamura, 1996). Its total radiated power and peak heat flux will reach 10.7 kW and 451 kW $mrad^{-2}$, respectively, when the undulator gap is set to be minimum. If such a very intensive undulator beam irradiates an uncooled portion of the beamline component or an unexpected part beyond its cooling ability, serious problems will arise, resulting in vacuum failure. Each beamline component for such a high-heat-load undulator beamline should be designed so as to avoid such a problem.

One of the major functions of the front end for the SPring-8 undulator beamline is to reduce the heat load on the downstream beamline components and to avoid accidental irradiation onto an unexpected portion. The SPring-8 front end consists of many components (Sakurai *et al.*, 1995) and its typical length is about 33 m between the light source and the terminal Be window assembly, which isolates the ultrahigh vacuum of the storage ring from the high vacuum of the monochromator. Among those components, several are used to reduce the heat load by limiting the spatial size of the undulator beam or employing a filtering material such as graphite foil.

A fixed mask with a small circular exit aperture is located 21.3 m from the light source. Although its main function is to avoid the accidental irradiation, it cuts off the off-axis part of the undulator beam. In the normal operating condition of the undulator beamline the majority of the radiated power is handled by utilizing the pre-slit (Takahashi *et al.*, 1998) followed by the *XY*-slits assembly (XY-SLIT) (Oura *et al.*, 1998). The pre-slit, which is located 26.4 m from the source, has a 4 mm-diameter circular aperture as its exit and is equipped with precision linear actuators to allow the vacuum vessel to be moved into the optimum position. The pre-slit will absorb almost half of the radiated power but the residual power is still high enough to damage the downstream components. The XY-SLIT, whose centre is located 28.9 m from the source, has an adjustable aperture and can be manipulated into a variety of aperture shapes so as to enable most fundamental radiation photons to pass through the assembly but most waste photons to be shut off. Its aperture size should be determined from the viewpoint of protecting the downstream component, such as the front-end Be window assembly, which is utilized under direct irradiation.

In considering the criterion for the thermomechanical failure of the Be window in practical use, some experimental results provide useful information. Shen *et al.* (1989) have performed an experiment simulating the failure condition of the Be window by means of electron bombardment, showing that the 250 μm window breaks at a power level of 660 W, which corresponds to a maximum temperature on the window of about 633 K. Asaoka *et al.* (1992) have conducted an experiment on the direct irradiation of the undulator beam onto the Be window. They observed irreversible buckling due to thermal expansion and release of inner mechanical stress resulting in a slow vacuum leak at an absorbed power density exceeding $\sim$2 W mm^{-2}, at which the maximum temperature of the window was $\sim$673 K. They concluded that the thermomechanical failure occurred when the temperature difference between the window centre and its peripheral edges exceeded $\sim$473 K, which was in good agreement with a simple maximum shearing stress theory for the failure condition.

In this article, we describe systematic studies on the allowable aperture size of the front end, namely the XY-SLIT, based on the results of the finite-element method. The heat load on the Be window is calculated as a function of the aperture size of the XY-SLIT, the thickness of the graphite filter and the deflection parameter K of the insertion device. ANSYS finite-element analysis is conducted to understand the thermal and thermomechanical properties of the window, and the failure criterion is discussed.

2. Finite-element model of the Be window

The Be window is a 250 μm-thick foil brazed onto a water-cooled Cu holder and the window opening is 10 mm in diameter. A couple of these windows and the ion pump attached to the middle section between two windows constitute the Be window assembly. The inner diameter of the cooling channel of the Cu holder is 6 mm and the average flow rate of the water has been measured to be in excess of 5 l min^{-1}.

An ANSYS finite-element model was formed for the quadrant structure of the Be window. We assumed a convective heat-transfer coefficient of 12000 W m^{-2} K^{-1} and a water temperature of 303 K in conservative calculations. The constant thermal conductivity of 134 W m^{-1} K^{-1} for Be was consistently used for the present analyses. Strictly speaking, a temperature-dependent value should be used, but the thermal conductivity employed is for the condition at 573 K and this results in a severe estimation in the temperature range below 573 K. We did not take account of thermal radiation cooling for the Be foil because we have concluded from the preliminary calculation that it is not so effective in the range of temperature for the present analyses

† Present address: Ishikawajima-Harima Heavy Industries Co. Ltd, 1 Shin-Nakahara-cho, Isogo-ku, Yokohama, Kanagawa 235, Japan.

Table 1
Material properties used in the analyses.

	Be	Cu
Thermal conductivity (W m^{-2} K^{-1})	134	383
Thermal expansion coefficient (10^{-6} K^{-1})	13	16.5
Young's modulus (GPa)	290	130
Poisson ratio	0.07	0.34

even if it is under the most severe case. Thermal and mechanical properties used in the analyses are listed in Table 1.

3. Absorbed power distribution

The finite-element analyses were preceded by estimating the absorbed power distribution in the window. For this purpose, the spectral and angular distributions of the undulator beam were calculated by using the computer code *SPECTRA* (Kitamura & Tanaka, 1996). The spatial distribution of the fundamental radiation in the horizontal (σ_x) and vertical (σ_y) directions at the location of the XY-SLIT was deduced from these computations so as to accept more than 68% photons of fundamental radiation. Deduced parameters of the spatial distribution and the aperture sizes used in the analyses are summarized in Table 2. Each acceptance A_x (horizontal) and A_y (vertical), the product of A_x and A_y being the aperture size, was chosen to be in units of the corresponding spatial distribution (σ_x and σ_y) and the six aperture sizes were determined for the analyses by keeping the ratio A_x/A_y constant. If we set the aperture size to $36R\sigma_y^2$, almost all photons of fundamental radiation pass through the aperture. In the normal operating mode of the beamline, however, setting the aperture size beyond $36R\sigma_y^2$ has no advantage even if the Be window withstands the heat load passing through the XY-SLIT.

The total absorbed power, P_T, in the foil is approximated by integrating all non-transmitted photons through the foil in which we assumed that Compton-scattered photons are also absorbed in the foil. This assumption gives rise to an overestimation of about 10% in the total absorbed power and a rigorous analysis needs to incorporate the Monte Carlo simulation.

In order to determine the spatial distribution of the absorbed power in the window, a number of off-axis photon-flux-density spectra were computed and those of the absorbed power density were calculated in the same manner as mentioned above. These results were adopted in the fitting procedure using the following equation,

$$F(h, v) = (2^{1/2}/\pi^{3/2})(P_T/\sigma H)\exp(-v^2/2\sigma^2)(1 - h^2/H^2)^{1/2}\,\delta(h, v),$$

where h and v are the horizontal and vertical distances, respectively, measured from the centre of the window, σ is the standard deviation of the spatial distribution of the absorbed power in the vertical direction, H is the half width of the spatial distribution of the absorbed power in the horizontal direction, $\delta(h, v)$ is the δ-function which becomes unity when the coordinate (h, v) resides in the projection of the aperture size of the XY-SLIT on the window. The absorbed power in the window as a function of the aperture size of the XY-SLIT, the thickness of the filter and the deflection parameter K are calculated using obtained parameters, at which the XY-SLIT is assumed to be located at 30 m from the source.

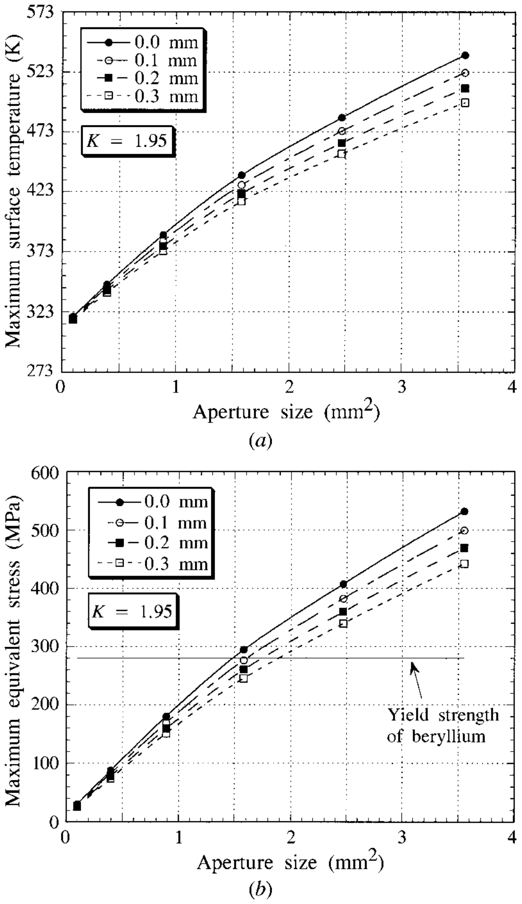

Figure 1
Maximum surface temperature (*a*) and maximum equivalent stress (*b*) in the Be window for K = 1.95, as a function of the aperture size of the XY-SLIT and the filter thickness. Curves in the figure are guides to the eye.

4. Results and discussion

The results from a series of ANSYS calculations are summarized in Table 3. Figs. 1(*a*) and 1(*b*) show, respectively, the typical results of the maximum surface temperature and the maximum equivalent stress, *i.e.* Mizes's equivalent stress, in the window for K = 1.95 as a function of aperture size. In order to determine the allowable aperture size of the front end, we have employed the following highly conservative criterion to avoid thermo-

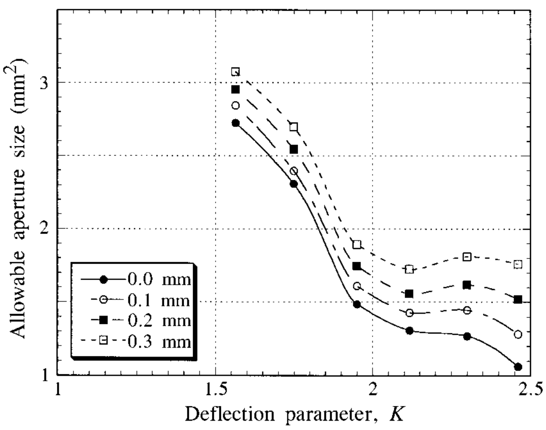

Figure 2
Deduced allowable aperture size of the XY-SLIT as a function of the deflection parameter and the filter thickness. Curves in the figure are guides to the eye.

Table 2
Parameters of the spatial distribution of the fundamental radiation and the aperture size of the XY-SLIT for different deflection parameter.

R is the ratio between σ_x and σ_y.

	Spatial distribution (mm)		Aperture size (mm^2)						
K	σ_x	σ_y	$R\sigma_y^2$	$4R\sigma_y^2$	$9R\sigma_y^2$	$16R\sigma_y^2$	$25R\sigma_y^2$	$36R\sigma_y^2$
1.564	0.522	0.177	0.092	0.370	0.831	1.478	2.310	3.326
1.749	0.519	0.183	0.095	0.380	0.855	1.520	2.374	3.419
1.95	0.522	0.189	0.099	0.395	0.888	1.579	2.467	3.552
2.117	0.525	0.195	0.102	0.409	0.921	1.638	2.559	3.685
2.3	0.528	0.201	0.106	0.425	0.955	1.698	2.653	3.821
2.461	0.528	0.210	0.111	0.443	0.998	1.774	2.772	3.991

Table 3
Maximum surface temperature and maximum equivalent stress as a function of aperture size and filter thickness.

	Filter	Maximum surface temperature (°C)						Maximum equivalent stress (MPa)					
K	(μm)	$R\sigma_y^2$	$4R\sigma_y^2$	$9R\sigma_y^2$	$16R\sigma_y^2$	$25R\sigma_y^2$	$36R\sigma_y^2$	$R\sigma_y^2$	$4R\sigma_y^2$	$9R\sigma_y^2$	$16R\sigma_y^2$	$25R\sigma_y^2$	$36R\sigma_y^2$
1.564	0	39.12	57.66	83.69	113.61	140.38	176.38	17.2	56.6	114	183	246	332
	100	38.84	56.81	82.00	110.90	136.68	171.31	16.7	54.9	111	177	238	320
	200	38.59	56.04	80.47	108.45	133.36	166.76	16.2	53.3	108	172	231	310
	300	38.36	55.32	79.03	106.14	130.20	162.44	15.7	51.8	105	167	223	300
1.749	0	40.61	60.96	90.42	125.95	158.07	197.42	20.0	63.4	129	210	286	380
	100	40.39	60.31	89.07	123.62	154.71	192.68	19.6	62.1	126	205	278	368
	200	39.99	59.12	86.70	119.75	149.40	185.53	18.9	59.7	121	197	266	352
	300	39.62	58.03	84.53	116.19	144.49	178.90	18.2	57.4	116	189	255	337
1.95	0	46.03	72.72	114.06	163.78	211.95	264.01	30.3	87.7	180	294	407	532
	100	45.10	70.21	109.06	155.71	200.79	249.41	28.5	82.6	169	276	382	499
	200	44.26	67.96	104.58	148.47	190.78	236.29	26.9	77.9	159	260	359	469
	300	43.51	65.93	100.54	141.93	181.70	224.36	25.5	73.8	151	245	339	442
2.117	0	47.60	79.03	125.44	185.45	234.29	298.17	33.2	101	204	342	458	609
	100	46.28	75.33	118.12	173.33	218.03	276.43	30.7	93.3	189	315	421	559
	200	45.13	72.11	111.78	162.78	203.87	257.46	28.6	86.7	175	292	389	516
	300	44.14	69.31	106.24	153.59	191.53	240.94	26.7	80.9	163	271	361	478
2.3	0	49.08	82.78	131.67	192.61	252.40	317.38	36.0	109	219	357	499	654
	100	47.20	77.53	121.68	175.92	229.10	286.64	32.5	98.0	196	320	446	583
	200	45.70	73.35	113.45	162.57	210.40	261.92	29.7	89.4	179	291	404	527
	300	44.48	69.94	106.78	151.67	195.13	241.72	27.4	82.3	164	267	369	480
2.461	0	52.42	96.52	154.42	222.18	305.28	382.60	42.3	137	267	422	618	804
	100	49.36	87.41	137.27	195.45	266.56	332.46	36.6	119	230	364	531	689
	200	47.00	80.37	123.99	174.71	236.48	293.45	32.1	104	201	318	463	600
	300	45.14	74.83	113.54	158.39	212.77	262.68	28.6	92.5	179	282	410	529

mechanical failure of the window: Mizes's equivalent stress should not exceed the yield strength of Be (280 MPa) since, if the maximum stress in the window exceeds the yield strength, plastic deformation and fatigue in the window will arise and result in a diminution of the life-cycle of the window.

The deduced allowable aperture sizes of the XY-SLIT are depicted as a function of the K parameter and the filter thickness in Fig. 2. The corresponding maximum temperatures of the window range between 423 and 433 K. These values are lower than those estimated by the simple maximum shearing stress theory and are enough to use the Be window in safety. According to the present analyses, we can set an upper limit of the aperture size of the XY-SLIT to be 3.11 (H) $\times$ 1.03 (V) mm. The practical aperture size, however, should be determined by taking account of the acceptance of the first optical component and its cooling ability. For example, at the condition of $K = 1.95$ and no filter, the allowable aperture size estimated by the present analyses is 2.03 (H) $\times$ 0.73 (V) mm. In this case, the transmitted photon flux of fundamental radiation and the transmitted power through the XY-SLIT can be calculated as almost 70% of the total photon flux and 1.03 kW, respectively.

The present results are only based on the elastic analysis. The analysis will have to be extended to take account of buckling phenomena. Further study is in progress.

References

Asaoka, S., Maezawa, H., Kamiya, Y. & Yanagihara, M. (1992). *Rev. Sci. Instrum.* **63**, 473–476.

Kitamura, H. (1996). *Hoshakou*, **9**, 403–412. (In Japanese.)

Kitamura, H. & Tanaka, T. (1996). *SPECTRA. Synchrotron Radiation Calculation Program*. Version 1.1 for Windows 3.2. Insertion Device Group, SPring-8, Hyogo 678-12, Japan.

Oura, M., Sakurai, Y. & Kitamura, H. (1998). *J. Synchrotron Rad.* **5**, 606–608.

Sakurai, Y., Oura, M., Sakae, H., Usui, T., Kimura, H., Oikawa, Y., Kitamura, H., Konishi, T., Shiwaku, H., Nakamura, A., Amamoto, H. & Harami, T. (1995). *Rev. Sci. Instrum.* **66**, 1771–1773.

Shen, Q., Bedzyk, M. J., Keeffe, M. J. & Schildkamp, W. (1989). *Rev. Sci. Instrum.* **60**, 1464–1467.

Takahashi, S., Sakurai, Y. & Kitamura, H. (1998). *J. Synchrotron Rad.* **5**, 581–583.